

Effects of chemical pressure on the charge-transfer spectra of CuX_4^{2-} complexes formed in Cu^{2+} -doped A_2MX_4 (M = Zn, Mn, Cd, Hg; X = Cl, Br)

This article has been downloaded from IOPscience. Please scroll down to see the full text article.

1998 J. Phys.: Condens. Matter 10 9525

(<http://iopscience.iop.org/0953-8984/10/42/017>)

View [the table of contents for this issue](#), or go to the [journal homepage](#) for more

Download details:

IP Address: 171.66.16.210

The article was downloaded on 14/05/2010 at 17:38

Please note that [terms and conditions apply](#).

Effects of chemical pressure on the charge-transfer spectra of CuX_4^{2-} complexes formed in Cu^{2+} -doped A_2MX_4 ($\text{M} = \text{Zn, Mn, Cd, Hg}$; $\text{X} = \text{Cl, Br}$)

R Valiente and F Rodríguez

DCITIMAC, Facultad de Ciencias, Universidad de Cantabria, 39005 Santander, Spain

Received 1 June 1998

Abstract. This work investigates the charge-transfer spectra of CuCl_4^{2-} and CuBr_4^{2-} complexes formed in anisotropic A_2MX_4 ($\text{X} = \text{Cl, Br}$) crystals. Attention is paid to the variations of the charge-transfer transition energies induced by chemical pressure effects when substituting $\text{Mn} \rightarrow \text{Zn} \rightarrow \text{Cd} \rightarrow \text{Hg}$ along the crystal series. A salient feature of this study is the weak sensitivity of these bands to structural changes of the complex in comparison to the sensitivity of the corresponding crystal field (d-d) bands. The knowledge of these structural-induced shifts is important since they are responsible to a great extent for the thermo- and piezochromic properties exhibited by some compounds containing CuX_4^{2-} units as chromophores. We present a tentative model based on a perturbed tetrahedral CuX_4^{2-} complex for explaining the weak sensitivity exhibited by the charge-transfer transitions in the title compounds. Furthermore the estimates of this model can also explain the big difference between the energy shift of d-d and charge-transfer transitions due to structural changes of the CuCl_4^{2-} complex in pure chlorocuprates.

1. Introduction

Ligand to metal charge transfer (LMCT) transitions in CuX_4^{2-} complexes ($\text{X} = \text{Cl, Br}$) play a relevant role in the optical properties of copper halides since they are mainly responsible for the colour and the dichroism of these compounds. This is particularly important for CuBr_4^{2-} because the charge-transfer (CT) spectra spread over the whole visible range. The knowledge of how CT spectra depend on the local structure around Cu^{2+} as well as on the complex orientation within the crystal is noteworthy since it allows us to explain the changes of colour exhibited by these systems upon structural changes of the complex induced either by temperature (thermochromism) or pressure (piezochromism).

Some pure copper(II) compounds such as $[(\text{C}_2\text{H}_5)_2\text{NH}_2]_2\text{CuCl}_4$ [1], $(\text{nmpH})_2\text{CuCl}_4$ [2] and $[(\text{CH}_3)_2\text{CHNH}_3]_2\text{CuCl}_4$ [3] show thermochromism associated with structural changes of CuCl_4^{2-} at phase transition temperatures, which are related to geometrical distortions of the complex from a nearly tetrahedral coordination to the square planar situation. Such structural modifications are accompanied by strong changes in both the crystal field (CF) and CT bands, whose shifts determine the occurrence of a given crystal colour. Although correlation studies between the CF spectra and the complex structure have been carried out along an ample series of pure copper compounds containing CuCl_4^{2-} units with different distortion Cl–Cu–Cl angles [3–7], that correlation however has been performed for neither

the CT spectra of CuCl_4^{2-} nor the CF (and also CT) of CuBr_4^{2-} . The lack of structural correlation with the CT spectra in both types of complex is presumably due to difficulties in obtaining the corresponding CT absorption spectra in concentrated materials because of the high oscillator strength of these transitions ($f \sim 0.1\text{--}0.01$) in comparison to the CF ones ($f \sim 10^{-4}$) [8, 9]. Besides that, the scarce number of pure copper bromides containing CuBr_4^{2-} units with different structural distortions is also a serious limitation to make correlations in CuBr_4^{2-} . Consequently, efforts devoted to accomplish such correlations are necessary in order to understand the variations experienced by the optical properties of materials upon structural changes.

The aim of this work is to investigate the effect of chemical pressure on the CT spectra of CuCl_4^{2-} and CuBr_4^{2-} formed in Cu^{2+} -doped A_2MX_4 ($\text{A} = \text{Cs}, (\text{CH}_3)_4\text{N}$; $\text{X} = \text{Cl}, \text{Br}$) along the series $\text{M} = \text{Mn} \rightarrow \text{Zn} \rightarrow \text{Cd} \rightarrow \text{Hg}$. The cationic substitution provides a range of metal–ligand distances for MX_4^{2-} from 2.23 to 2.45 Å in chlorides whereas from 2.44 to 2.59 Å in bromides for accommodating substitutional Cu^{2+} at the tetrahedral sites. In terms of pressure it means a hydrostatic local pressure of about 100 kbar assuming that the local bulk modulus is 300 kbar for both complexes.

2. Experiment

Single crystals of Cu^{2+} -doped $\text{TMA}_2\text{HgCl}_4$, Cs_2ZnCl_4 and $\text{TMA}_2\text{HgBr}_4$ were grown by slow evaporation at 40 °C from HCl or HBr acidic aqueous solutions containing a 2:1 stoichiometric ratio of the corresponding tetramethylammonium (TMA) or caesium halide and the metallic halide, respectively. Single crystals $\text{TMA}_2\text{MnCl}_4$ and $\text{TMA}_2\text{CdBr}_4$ were grown as indicated in [9–11]. A molar 1–10 mol% of CuCl_2 or CuBr_2 was added to the solutions in each case.

The room temperature *Pmcn* orthorhombic structure was checked by x-ray diffraction. Several plates of each crystal were selected for optical studies with the aid of a polarizing microscope. The spectra were recorded with a Lambda 9 Perkin Elmer spectrophotometer equipped with Glan Taylor polarizing prisms. Sample thicknesses for absorption were about 0.2–0.5 mm depending on the Cu concentration of the sample. The temperature was varied in the 10–300 K range with a Scientific Instruments 202 closed-circuit cryostat and an APD-K controller.

3. Results and discussion

3.1. Polarized optical absorption spectra of CuCl_4^{2-} and CuBr_4^{2-}

Figures 1 and 2 show the polarized optical spectra of the Cu^{2+} -doped A_2MCl_4 and A_2MBr_4 crystal series at low temperature, respectively. The spectra are similar to the CT spectra obtained 30 years ago from diluted non-aqueous solutions of CuCl_4^{2-} and CuBr_4^{2-} ions [12, 13] as well as those recently obtained from solid solutions whose polarization measurements allowed a complete spectrum assignment on the basis of a D_{2d} perturbed tetrahedral symmetry [9, 11, 14]. The band structure shown by both types of complex consists basically of two structured bands denoted by A and B, and a single band in the high energy side of the spectrum denoted by C placed, respectively, around 24 500, 33 500 and 42 000 cm^{-1} in CuCl_4^{2-} and 18 000, 28 500 and 36 500 cm^{-1} in CuBr_4^{2-} (table 1). Following the procedure established in [9, 11, 14], the analysis of the spectrum anisotropy indicates that bands A and B are *x*, *y*-polarized while band C is *z*-polarized according to the crystal field distortion of D_{2d} symmetry exhibited by the tetracoordinated CuX_4^{2-}

Table 1. Peak energies corresponding to the charge transfer bands of CuCl_4^{2-} and CuBr_4^{2-} complexes obtained from the $T = 10$ K optical absorption spectra of figures 1 and 2. Peak labelling is given according to the assignment of figure 3. Data for the Cu^{2+} -doped $\text{TMA}_2\text{MnCl}_4$, $\text{TMA}_2\text{MnBr}_4$ and $\text{TMA}_2\text{CdBr}_4$ are taken, respectively, from [9, 14, 11]. Units in cm^{-1} .

	$\text{TMA}_2\text{MnCl}_4$: Cu^{2+}	C_2ZnCl_4 : Cu^{2+}	$\text{TMA}_2\text{HgCl}_4$: Cu^{2+}	$\text{TMA}_2\text{ZnBr}_4$: Cu^{2+}	$\text{TMA}_2\text{CdBr}_4$: Cu^{2+}	$\text{TMA}_2\text{HgBr}_4$: Cu^{2+}
	Peak energy (cm^{-1})	Peak energy (cm^{-1})	Peak energy (cm^{-1})	Peak energy (cm^{-1})	Peak energy (cm^{-1})	Peak energy (cm^{-1})
(A1)				16880	16780	16770
(A2)	24420	24530	24420	18010	17920	17890
(A3)				19300	19200	19160
(C')	~29400	29240	29250	23350	23500	23200
(B1)				25350	25250	25250
(B2)	33700	33780	33650	27300	27000	27300
(B3)				28950	28900	28800
(C)	41330	42550	—	36700	36400	—

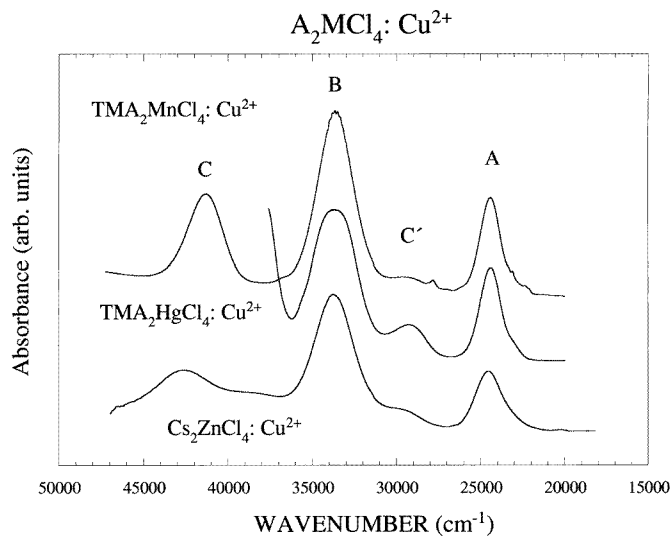


Figure 1. Polarized optical absorption spectra of single crystals of Cu^{2+} -doped TMA_2MnCl_4 , TMA_2HgCl_4 and Cs_2ZnCl_4 taken with E along one of the extinction directions at $T = 10$ K. The small peaks observed around $22\,000$ and $28\,000\text{ cm}^{-1}$ in Cu^{2+} -doped TMA_2MnCl_4 correspond to Mn^{2+} . The peak assignment is shown in figure 3. The optical absorption for the mercurate is scanned below $38\,000\text{ cm}^{-1}$ due to the absorption background of the host crystal.

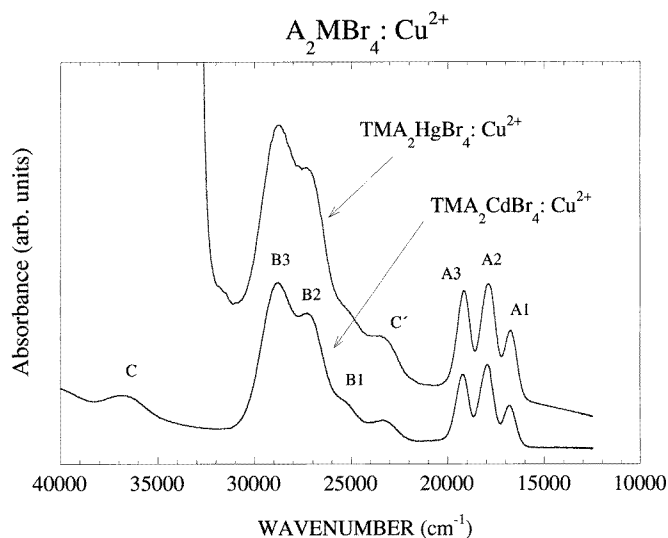


Figure 2. Polarized optical absorption spectra of single crystals of Cu^{2+} -doped TMA_2HgBr_4 and TMA_2CdBr_4 taken with E along one extinction direction at $T = 10$ K. Note the triplet structure displayed by the first band. The optical absorption for the mercurate is scanned below $33\,000\text{ cm}^{-1}$ due to the absorption background of the host crystal.

complexes by the Jahn–Teller (JT) effect. In fact this distortion is associated with the flattening of the X–Cu–X bond angle, θ , along one of the three S_4 axes of the tetrahedron; i.e. electron–phonon coupling with the JT active vibrational bending mode of e symmetry.

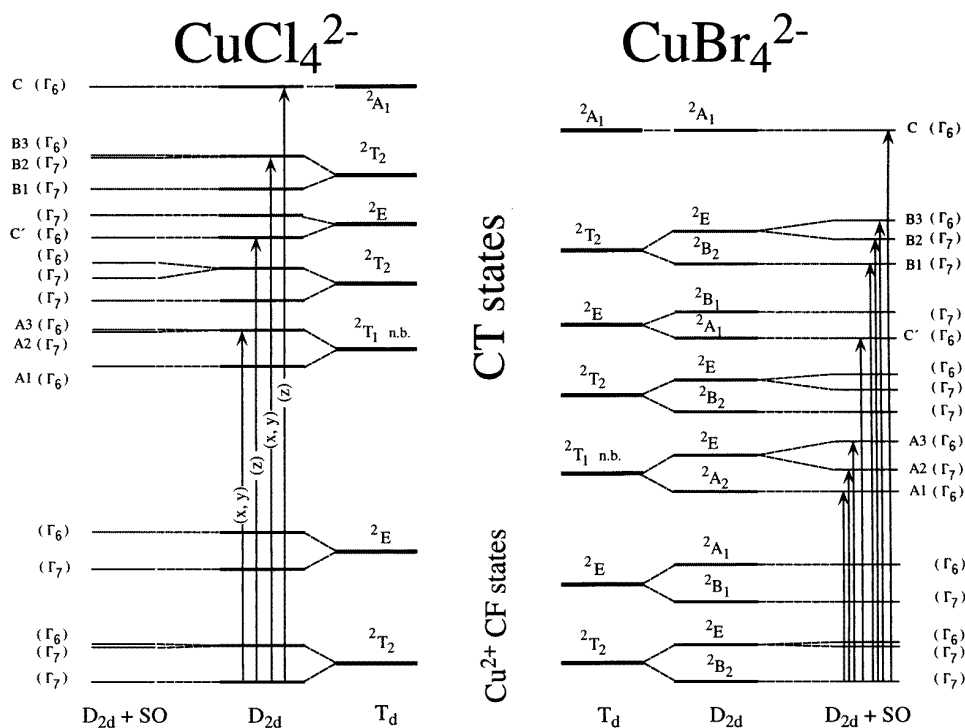


Figure 3. Schematic state diagram corresponding to the CuCl_4^{2-} and CuBr_4^{2-} complexes showing the assigned electronic transitions on the basis of a crystal field distortion of D_{2d} symmetry and the spin-orbit interaction of the ligands. Within D_{2d} the electric dipole allowed transitions correspond to ${}^2E \rightarrow {}^2B_2$ and to ${}^2A_1 \rightarrow {}^2B_2$, which are x , y and z polarized, respectively. When the spin-orbit interaction of the ligand is included, the double group representation in D_{2d} allows transitions $\Gamma_7 \rightarrow \Gamma_6$ (x , y , z polarized) and $\Gamma_7 \rightarrow \Gamma_7$ (x , y polarized). The triplet structure of the CuBr_4^{2-} complexes is explained in this scheme.

Within D_{2d} , bands A and B thus correspond to electronic transitions from the mainly ligand π -bonding and σ -bonding orbitals of e symmetry to the mainly Cu^{2+} $b_2(x^2 - y^2)$ orbital, respectively, according to the selection rules for the electric dipole transitions in this symmetry. On the other hand the z -polarized C band corresponds to the CT transition from the σ -bonding a_1 ligand orbital to b_2 . Figure 3 shows a schematic energy state diagram of CuX_4^{2-} in D_{2d} symmetry including the spin-orbit interaction of the X^- ligands where the observed transitions are indicated by arrows. Upon replacing Cl^- by Br^- two important facts must be underlined: (i) the overall spectrum shifts 5000–6000 cm^{-1} to lower energies according to Jørgensen's scale given the different optical electronegativity of these two ligands ($\Delta\chi = 0.2$) [15]. (ii) Bands A and B in CuBr_4^{2-} display a triplet structure which is associated with the spin-orbit interaction of the Br ligands ($\xi_{4p} = 2098 \text{ cm}^{-1}$) [11, 13, 14]. Indeed the three components of the band denoted by subscripts 1, 2 and 3 are related to the splitting of the parent tetrahedral t_1 and t_2 orbitals by the combined effect of the ligand spin-orbit interaction and the D_{2d} crystal field as figure 3 shows. However this splitting is not observed in CuCl_4^{2-} due to the weaker spin-orbit coupling of the Cl ligand ($\xi_{3p} = 500 \text{ cm}^{-1}$). The transition energies of the CT bands for the two investigated crystal series are collected in table 1.

Concerning pressure effects, the present results point out that the CT bands A and B are not very sensitive to changes of chemical pressure either for CuCl_4^{2-} or for CuBr_4^{2-} . Actually the CT transition energy, that can be accurately measured in CuBr_4^{2-} by the narrow band structure in A, shifts less than 200 cm^{-1} along the series (table 1). A similar situation is observed for CuCl_4^{2-} .

Although we are not able to distinguish in the case of Cu^{2+} impurities whether the CuX_4^{2-} complex exhibits structural modifications along the series or whether the complex structure remains unchanged, we will analyse the shifts of the CT bands in comparison to the CF ones in these two extreme situations. If the geometry of the CuX_4^{2-} impurities is the same along the crystal series, i.e. it does not depend on the size of the host MX_4^{2-} tetrahedron as demonstrated for the CuCl_4^{2-} complex formed in Cu^{2+} -doped $[(\text{CH}_3)_4\text{N}]_2\text{MnCl}_4$ [9], then both CF and CT bands, strongly dependent on the CuX_4^{2-} complex structure, will not shift along the series, thus explaining the weak sensitivity of the CT bands. In the more probable case that a structural modification of CuX_4^{2-} takes place along the series, the lack of sensitivity of CT bands A and B to structural changes can be explained if we assume that complex distortions induced by pressure tend to reduce the dihedral X–Cu–X angle toward the square-planar situation ($\theta = 180^\circ$) when the X–Cu distance increases or vice versa. This type of distortion is based on geometrical arguments taking into account that the two extreme configurations the complex can adopt just correspond to the tetrahedron ($\theta = 109.5^\circ$) and the square-planar coordination ($\theta = 180^\circ$). The associated bond distances would be $R_{\text{X-Cu}} = r_{\text{X}} + r_{\text{Cu}}$ and $R_{\text{X-Cu}} = \sqrt{2}r_{\text{X}}$, respectively, whenever the ionic radii of the ligand, r_{X} , and the metal, r_{Cu} , verify the inequality $\sqrt{2}r_{\text{X}} > r_{\text{X}} + r_{\text{Cu}} > \sqrt{3/2}r_{\text{X}}$ so that $4.4r_{\text{Cu}} > r_{\text{X}} > 2.4r_{\text{Cu}}$. This condition is fulfilled for CuCl_4^{2-} and CuBr_4^{2-} where $r_{\text{Cl}} = 1.81\text{ \AA}$, $r_{\text{Br}} = 1.95\text{ \AA}$ and $r_{\text{Cu}} = 0.57\text{ \AA}$. Therefore intermediate configurations of the complex associated with θ values from 109.5 to 180° must correspond to Cu–X distances from $r_{\text{X}} + r_{\text{Cu}}$ to $\sqrt{2}r_{\text{X}}$ within a rigid sphere model. We have verified that this effect occurs not only in Cu^{2+} impurities [9] but also in pure copper compounds as indicated in the next section.

3.2. Structural correlations in CuCl_4^{2-} : crystal field and charge transfer spectra

There is a great number of pure chlorocuprates providing a wide range of Cu–Cl distance ($R = 2.22\text{ \AA}$ – 2.27 \AA) and Cl–Cu–Cl distortion angle ($\theta = 110^\circ$ – 180°) that allows us to establish structural correlations in tetracoordinated CuCl_4^{2-} complexes. Figure 4 plots the distortion angle, θ , obtained from x-ray diffraction for a series of compounds having CuCl_4^{2-} units as a function of the corresponding Cu–Cl bond length, R . It must be noted that there is a clear correlation between θ and R along the chlorocuprate series available in the literature ([3–7] and references therein). The observed linear behaviour between θ and R , as $\theta (^\circ) = -2585 + 1215R (\text{\AA})$, justifies the proposed model for copper complexes. Apart from this structural correlation, there is also the well known correlation between the CF spectra of these compounds and the distortion angle, θ , as has been pointed out elsewhere [3–7]. The variation of the maximum corresponding to the high energy CF band with θ shown in figure 5 illustrates this behaviour. The blue shift experienced by the CF band upon increasing θ is a direct consequence of the enhancement of the Jahn–Teller distortion on the complex. The higher θ is the bigger the CF splitting, and consequently the higher the transition energy as is shown in figure 3. This narrow relation between E and θ was already exploited to extract structural information about CuCl_4^{2-} impurities through the corresponding CF spectrum [9].

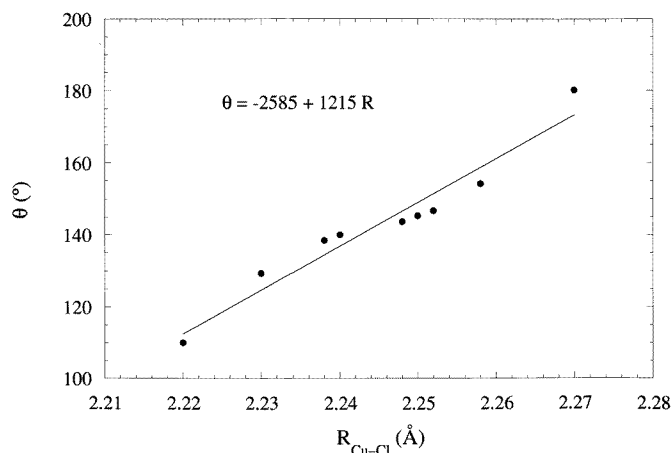


Figure 4. Plot of the D_{2d} distortion angle, θ , versus the equilibrium Cu–Cl bond distance, R , for CuCl_4^{2-} complexes. The θ and R values have been obtained from structural data along a series of pure chlorocuprates [3–9]. The straight line represents the least-squares fit to the data.

An analysis of the variation of the different CF transitions with θ within the atomic overlap model (AOM) has been given elsewhere [16]. This analysis provides a self-consistent way of parametrizing the transition energies as a function of θ . Figure 5 also includes a plot of the individual transition energies associated with the different CF transitions with θ . From this plot we found that the variation of the first CF band $e \rightarrow b_2$ around the tetrahedral symmetry ($\theta = 109.5^\circ$) is $\partial E_{CF}(e \rightarrow b_2)/\partial \theta = 250 \text{ cm}^{-1}/^\circ$. This value just represents the variation of the pure JT splitting of the parent tetrahedral t_2 orbital by D_{2d} distortions.

Nevertheless there has been no similar investigation devoted to correlating the variations of the CT bands with θ . The reason for this presumably lies in the high oscillator strengths of the CT bands ($f \sim 0.1\text{--}0.01$) in comparison to the CF ones ($f \sim 10^{-4}$) making the CF spectrum easier to obtain in pure compounds.

A relevant aspect concerning the variations undergone by the first CF $e \rightarrow b_2$ transition, and the corresponding first CT transition, is the different sensitivity of the associated two bands to structural changes of the complex. While the CF energy only depends in a first approximation on the JT distortion, θ , the CT energy depends on both parameters R and θ . This aspect is noteworthy to understand the origin of the different sensitivity, if we consider that the partial derivatives, $[\partial E_{CT}(e \rightarrow b_2)/\partial \theta]_R$ and $[\partial E_{CT}(e \rightarrow b_2)/\partial R]_\theta$, may have opposite signs. In order to illustrate this situation figure 6 depicts the energy level diagram of a CuX_4^{2-} complex in tetrahedral symmetry (R_0 , $\theta_0 = 109.5^\circ$), and for two different structures with (i) $R < R_0$ maintaining the T_d symmetry, and (ii) $R = R_0$ and $\theta > \theta_0$. In the first configuration both the energy separation between the tetrahedral split t_2 and e mainly d orbitals, as well as the CT $e \rightarrow b_2$ energy, increase upon an isotropic reduction of the Cu–X distances (totally symmetric a_1 distortion). In the second case, corresponding to a JT distortion of e_θ symmetry, the tetrahedral t_2 and e orbitals split but keeping each centre of gravity unshifted. This statement can be understood within a perturbative scheme, taking into account that the D_{2d} distortion crystal-field matrices associated with either triplets or doublets are traceless. Consequently, the sum of the D_{2d} -split energies for e or t_2 must be twice or three times the unperturbed energy, respectively (figure 6). Therefore the structural

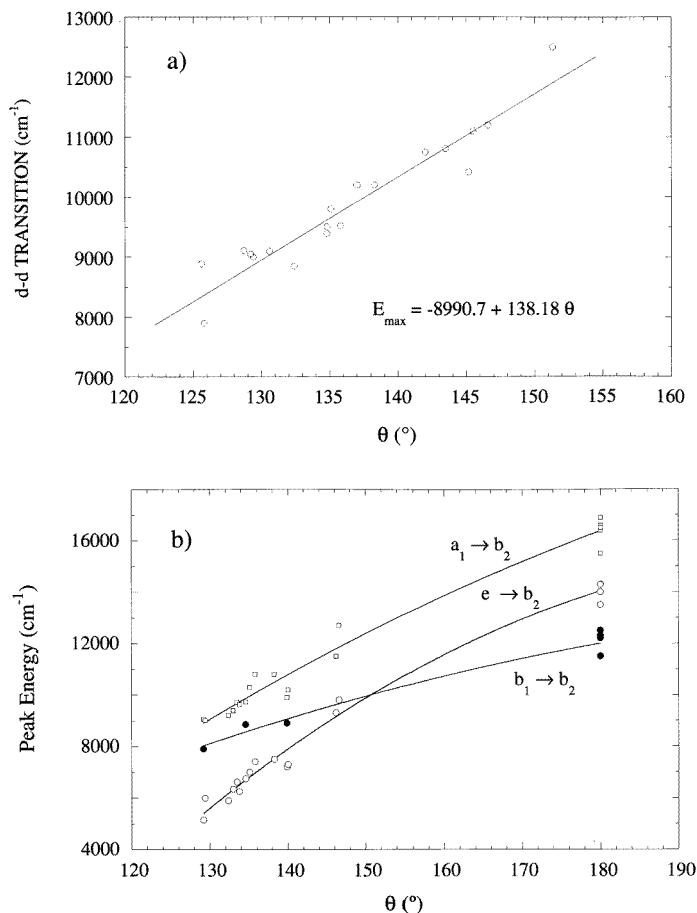


Figure 5. (a) Variation of the maximum corresponding to the high energy CF band obtained from the optical absorption spectra of pure chlorocuprates [3–7]. Note the linear behaviour between E and θ . The least-squares linear fit equation is given in the figure. (b) Variation of the individual transition energies corresponding to the three CF transitions in CuCl_4^{2-} . The curves represent the theoretical variations within the AOM model [16].

dependence of the CF or the CT energy in a perturbative scheme can be written as

$$\frac{\partial E(e \rightarrow b_2)}{\partial \theta} = [\frac{\partial E}{\partial \theta}]_R + [\frac{\partial E}{\partial R}]_{\theta} [\frac{\partial R}{\partial \theta}] \quad (1)$$

where derivatives are given at the equilibrium tetrahedral geometry, R_0 and θ_0 , and assuming that θ varies with R as in figure 4. Now depending on whether we consider the first CF $e \rightarrow b_2$ energy, E_{CF} , or the corresponding first CT energy, E_{CT} , we obtain a different shift. In the former case, $[\frac{\partial E_{CF}}{\partial R}]_{\theta} = 0$, and then $\frac{\partial E_{CF}}{\partial \theta} = [\frac{\partial E_{CF}}{\partial \theta}]_R = 250 \text{ cm}^{-1}/^\circ$ ([16] and references therein), indicating that the first CF transition energy only depends on the JT distortion. For CT transitions however both terms contribute to the shift, and thus CT transitions in general are expected to be more sensitive than the CF ones. The spectroscopic study performed on the so-called centre II, $\text{CuCl}_4(\text{NH}_3)_2$, formed in Cu^{2+} -doped NH_4Cl crystals is an example of this behaviour [17].

Nevertheless this situation, illustrated in figure 6, is not the present one since a negative value of $[\frac{\partial E_{CT}}{\partial R}]_{\theta}$ leads to opposite contributions in the right hand side of

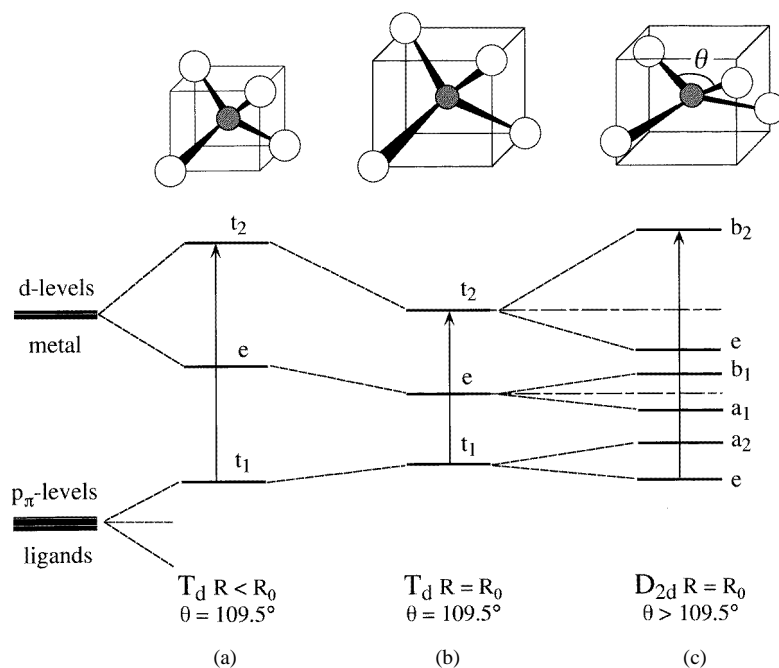


Figure 6. Approximate energy level diagram of a CuX_4^{2-} complex including the mainly Cu^{2+} d orbitals as well as the first charge transfer mainly ligand π orbitals. The diagram is given for three different complex configurations: (a) For the equilibrium tetrahedral geometry, R_0 and $\theta_0 = 109.5^\circ$. (b) A totally symmetric (a_1) crystal field distortion, $R < R_0$ and $\theta = \theta_0$. (c) A Jahn–Teller distortion of D_{2d} symmetry (e_θ mode), $R = R_0$ and $\theta > \theta_0$. Note that the centre of gravity of the tetrahedral t_2 and e orbitals do not shift for this type of distortion.

equation (1). Although there is no analogous correlation between CT energy and θ for the CuCl_4^{2-} complex, we can estimate the variation, $\partial E_{CT}/\partial\theta$, of equation (1) from multiple scattering (MS)– $X\alpha$ calculations carried out in CuCl_4^{2-} as a function of R [18] and θ [9]. The results of these calculations are $[\partial E_{CT}/\partial R]_\theta = -7 \times 10^4 \text{ cm}^{-1} \text{ \AA}^{-1}$ and $[\partial E/\partial\theta]_{R=2.25 \text{ \AA}} = 127 \text{ cm}^{-1}/^\circ$. These two values are consistent with the blueshift experienced by CT bands upon isotropic reduction of the metal–ligand distance (first term), while the positive value of the second term reflects the JT contribution to the energy shift of a CT transition involving an electronic jump between the two extreme levels of the split mainly ligand e orbitals and the t_2 orbitals of Cu^{2+} , respectively (figure 6). Taking the experimental value $[\partial R/\partial\theta] = 8 \times 10^{-4} \text{ \AA}/^\circ$ from figure 4, we obtain:

$$\partial E_{CT}/\partial\theta = 127 - 7 \times 10^4 \times 8 \times 10^{-4} = 70 \text{ cm}^{-1}/^\circ.$$

This value is about three or four times smaller than the $250 \text{ cm}^{-1}/^\circ$ value found for the first CF energy and therefore it reasonably explains the weak sensitivity of the CT bands in these materials to structural changes of the complex. Furthermore, the present estimates are also able to explain why the first CT band measured in some chlorocuprates, such as $(\text{nmpH})_2\text{CuCl}_4$ ($\theta = 180^\circ$ and $E_{CT} = 26\,400 \text{ cm}^{-1}$), $(\text{NPhpipzH}_2)\text{CuCl}_4$ ($\theta = 142^\circ$ and $E_{CT} = 27\,030 \text{ cm}^{-1}$) and $\text{TMA}_2\text{CuCl}_4$ ($\theta = 129.4^\circ$ and $E_{CT} = 25\,000 \text{ cm}^{-1}$), are less sensitive to variations of θ than the corresponding CF bands: $13\,600$, $10\,750$ and $9\,000 \text{ cm}^{-1}$, respectively [2–8].

4. Conclusions

We have developed a perturbative model for explaining the energy shifts of the CT and CF bands induced by structural distortions in tetrahedral CuX_4^{2-} complexes. A relevant conclusion is the weaker sensitivity of the CT bands in comparison to the CF bands to structural changes of the complex when both θ and R increase. The different behaviour exhibited by these bands is due to the opposite contribution to the CT shift from θ and R . However this is not the situation of the first CF band since it is associated with the Jahn–Teller splitting of the tetrahedral t_2 d levels, and therefore does not depend on R . The estimates of this model can explain the absence of CT shift upon chemical pressure along the $\text{A}_2\text{MX}_4:\text{Cu}^{2+}$ ($\text{X} = \text{Cl}, \text{Br}$) series presented here. The model is also able to explain the weak dependence of the CT transitions on θ variations from 129 to 180° observed experimentally in pure chlorocuprates.

Acknowledgments

This work was supported by Caja Cantabria and the CICYT (project No PB95-0581).

References

- [1] Bloomquist D R, Pressprich M R and Willett R D 1988 *J. Am. Chem. Soc.* **110** 7391
- [2] Harlow R L, Wells W J III, Watt G W and Simonsen S H 1975 *Inorg. Chem.* **14** 1768
- [3] Willett R D, Haugen J A, Lebsack J and Morrey J 1974 *Inorg. Chem.* **13** 2510
- [4] Harlow R L, Wells W J III, Watt G W and Simonsen S H 1974 *Inorg. Chem.* **13** 2106
- [5] Battaglia L P, Bonamartini Corradi A B, Marcotrigiano G, Menabue L and Pellacani G C 1979 *Inorg. Chem.* **18** 148
- [6] Halvorson K E, Patterson C and Willett R D 1990 *Acta Crystallogr. B* **46** 508
- [7] Bond M R, Johnson T J and Willett R D 1988 *Can. J. Chem.* **66** 963
- [8] Desjardins S R, Penfield K W, Cohen S L, Musselman R L and Solomon E I 1983 *J. Am. Chem. Soc.* **105** 4590
- [9] Marco de Lucas M C, Rodríguez F and Aramburu J A 1991 *J. Phys.: Condens. Matter* **3** 8945
- [10] Valiente R, Marco de Lucas M C, Espeso J I and Rodríguez F 1993 *Solid State Commun.* **86** 663
- [11] Valiente R, Marco de Lucas M C and Rodríguez F 1995 *J. Phys.: Condens. Matter* **7** 3881
- [12] Bird B D and Day P 1968 *J. Chem. Phys.* **49** 392
- [13] Ferguson J 1964 *J. Chem. Phys.* **40** 3406
- [14] Marco de Lucas M C and Rodríguez F 1993 *J. Phys.: Condens. Matter* **5** 2625
- [15] Jørgensen C K 1970 *Prog. Inorg. Chem.* **12** 101
- [16] Hitchman M A 1994 *Comments Inorg. Chem.* **15** 197
- [17] Breñosa A G, Moreno M, Rodríguez F and Couzi M 1991 *Phys. Rev. B* **44** 9859
- [18] Aramburu J A, Moreno M and Bencini A 1987 *Chem. Phys. Lett.* **140** 462